

## THE LOCATION OF SOLAR METRIC TYPE II RADIO BURSTS WITH RESPECT TO THE ASSOCIATED CORONAL MASS EJECTIONS

R. RAMESH<sup>1</sup>, M. ANNA LAKSHMI<sup>2</sup>, C. KATHIRAVAN<sup>1</sup>, N. GOPALSWAMY<sup>3</sup>, AND S. UMAPATHY<sup>2</sup>

<sup>1</sup> Indian Institute of Astrophysics, Bangalore 560034, India; ramesh@iiap.res.in

<sup>2</sup> School of Physics, Madurai Kamaraj University, Madurai 625021, India

<sup>3</sup> NASA Goddard Space Flight Center, Greenbelt, MD, USA

Received 2012 January 11; accepted 2012 March 31; published 2012 June 4

### ABSTRACT

Forty-one solar type II radio bursts located close to the solar limb (projected radial distance  $r \gtrsim 0.8 R_{\odot}$ ) were observed at 109 MHz by the radioheliograph at the Gauribidanur observatory near Bangalore during the period 1997–2007. The positions of the bursts were compared with the estimated location of the leading edge (LE) of the associated coronal mass ejections (CMEs) close to the Sun. 38/41 of the type II bursts studied were located either at or above the LE of the associated CME. In the remaining 3/41 cases, the burst was located behind the LE of the associated CME at a distance of  $<0.5 R_{\odot}$ . Our results suggest that nearly all the metric type II bursts are driven by the CMEs.

*Key words:* Sun: activity – Sun: corona – Sun: coronal mass ejections (CMEs) – Sun: flares – Sun: radio radiation – solar–terrestrial relations

### 1. INTRODUCTION

Solar type II radio bursts are the signatures of magneto-hydrodynamic (MHD) shocks propagating outward through the solar atmosphere. They frequently occur as two relatively slow drifting emission bands (fundamental (F) and harmonic (H)) with a frequency ratio of  $\approx 1:2$ . The frequency drift from high to low frequencies (typically  $\sim 0.5 \text{ MHz s}^{-1}$ ) results from the decrease of electron density ( $N_e$ ) with radial distance in the solar atmosphere. The observed drift rate can be converted into a velocity if the dependence of  $N_e$  on  $r$  is known. The characteristics and detailed description of solar type II bursts can be found in Nelson & Melrose (1985), Mann et al. (1995), Aurass (1997), and Gopalswamy (2006). In a longstanding and healthy debate, MHD shocks in the low corona ( $r \lesssim 2 R_{\odot}$ ) have been attributed to either solar flares or coronal mass ejections (CMEs) or some combination of the two (Gopalswamy 2006; Mann & Vršnak 2007; Pick & Vilmer 2008; Vršnak & Cliver 2008; Nindos et al. 2011). It is difficult to observe CMEs in this distance range due to observational constraints. In addition, because of the geometry of white-light scattering, CMEs occurring at the solar limb are much easier to detect in coronagraph images than those near the center of the solar disk (Cliver et al. 1999; Gopalswamy et al. 2001). The type II radio bursts occurring at metric wavelengths are considered to be the direct, and one of the earliest, signatures of shocks in the solar corona. Results obtained using radio spectral observations of metric type II bursts indicate that they can be explained by CME driven shocks (Lara et al. 2003; Cliver et al. 2004; Cho et al. 2005, 2007, 2008, 2011; Subramanian & Ebenezer 2006; Mancuso 2007; Gopalswamy et al. 2009a; Liu et al. 2009). Most of these works were carried out without positional information on the type II bursts. Radioheliograph data have positional information of the type II bursts. Therefore we can directly verify the spatial relationship with CMEs and flares using them. We would like to note here that type II bursts with positional information have been reported by several authors in the past (Dulk 1970; Stewart et al. 1974a, 1974b; Nelson & Robinson 1975; Kosugi 1976; Wagner & MacQueen 1983; Gergely et al. 1983; Gary et al. 1984; Gopalswamy & Kundu 1992; Maia et al. 2000; Magdalenic et al. 2010; Ramesh

et al. 2010; Nindos et al. 2011). These were studies of either a single event or a few selective events. The present work utilizes a comparatively larger data set (41 bursts) at a single frequency from solar cycle 23. We have spectral confirmation for all the type II bursts with positional information reported in this paper. All the events were accompanied by an X-ray/H $\alpha$  flare and white-light CME.

### 2. DATA SET

The type II bursts used in the present study were obtained at 109 MHz during 1997–2007 with the Gauribidanur radioheliograph (GRH; Ramesh et al. 1998) located about 100 km north of Bangalore in India.<sup>4</sup> The GRH is a T-shaped radio interferometer array dedicated to observations of the solar corona. The GRH has observed the Sun daily between  $\approx 4$ –9 UT since 1997. The angular resolution of the array at its zenith is  $\approx 7' \times 10'$  (R.A.  $\times$  decl.), and the minimum detectable flux is  $\approx 200 \text{ Jy}$  at the above frequency. The co-ordinates of the array are longitude =  $77^{\circ}27'07''$  east and latitude =  $13^{\circ}36'12''$  north. Though a large number of type II bursts was observed with the GRH during the above period, we specifically selected only those events located close to the solar limb (projected  $r \geq 0.8 R_{\odot}$ ) for the present work. This minimized possible projection effects. With this limitation, we could get 41 events during the period 1997–2007. We used data obtained with the Large Angle and Spectrometric Coronagraph (LASCO; Brueckner et al. 1995) on board *Solar and Heliospheric Observatory (SOHO)* for information on the associated white-light CMEs as listed in the CME catalog<sup>5</sup> (Gopalswamy et al. 2009b). The solar sources of the CMEs were identified as the location of the associated H $\alpha$  flares listed in the Solar Geophysical Data (SGD)<sup>6</sup> and further verified from the flare locations derived using the EUV images obtained with Extreme-ultraviolet Imaging Telescope (Delaboudiniere et al. 1995) on board *SOHO*.

Figure 1 shows a type II burst imaged by the GRH at 109 MHz around  $\approx 07:23 \text{ UT}$  on 2007 May 23 superposed on a LASCO

<sup>4</sup> <http://www.iiap.res.in/centers/radio>

<sup>5</sup> [http://cdaw.gsfc.nasa.gov/CME\\_list](http://cdaw.gsfc.nasa.gov/CME_list)

<sup>6</sup> <http://sgd.ngdc.noaa.gov/sgd/solarindex.jsp>



**Figure 1.** Composite of the radioheliogram of the type II burst of 2007 May 23 observed with the GRH at 109 MHz and the associated LASCO C2 difference image. Solar north is straight up and east is to the left. The inner white circle at the center represents the solar limb. The outermost gray circle indicates the occulting disk of the LASCO C2 coronagraph. Its radius is  $\approx 2.2 R_{\odot}$ . The bright white-light emission just above the southwest quadrant of the coronagraph occulter corresponds to a CME. The intense discrete radio source (shown by white contours) with its centroid at CPA  $\approx 262^{\circ}$  and  $r \approx 1.4 R_{\odot}$ , located between the aforementioned white-light structure and the solar limb, is a type II burst. It was observed at  $\approx 07:23$  UT, about 25 minutes before the first appearance of the white-light CME in the LASCO FOV (see Table 1 for details). The peak brightness temperature ( $T_b$ ) of the radio source is  $\approx 4 \times 10^8$  K. The contours are in interval of 10% of the peak  $T_b$  and the outermost contour corresponds to  $T_b \approx 1.2 \times 10^8$  K.

C2 difference image at  $\approx 07:48$  UT. Figure 2 shows the dynamic spectrum of the above type II burst at lower frequencies (85–25 MHz) as observed with the Gauribidanur Radio Spectrograph System (GRASS; Ebenezer et al. 2007). One can note the presence of both the fundamental and harmonic components in the spectrum. The frequency of operation of the GRASS is limited to the above range, hence the truncation of the spectrum at 85 and 25 MHz. A comparison of Figures 1 and 2 indicates that the discrete source of intense radio emission contours in Figure 1 at 109 MHz most likely corresponds to the harmonic type II burst as its fundamental component is clearly seen in the spectrum at 54.5 MHz in Figure 1 at the same time, i.e.,  $\approx 07:23$  UT. We confirmed this with the spectrum of the same event as observed with the CALLISTO radio spectrograph (Benz et al. 2005; Monstein et al. 2007) at the Gauribidanur observatory and the SGD reports. Note that the CALLISTO operates at frequencies  $\gtrsim 50$  MHz. We would like to add here that metric type II burst of 2007 May 23 is a typical example of events with starting frequency  $< 50$  MHz (Gopalswamy 2006). The projected radial distance  $r$  and the central position angle (CPA, measured counterclockwise from the solar north) of the centroid of the burst in Figure 1 are  $\approx 1.4 R_{\odot}$  and  $262^{\circ}$ , respectively. The radio burst was associated with a B5.3 soft X-ray flare observed by the X-ray sensor on board *Geostationary Operational Environmental Satellite* (GOES) from the heliographic location S10W51.<sup>7</sup> The onset of the X-ray flare was at  $\approx 07:15$  UT. An

inspection of the LASCO CME catalog revealed that a CME at CPA  $\approx 266^{\circ}$  and width  $\approx 77^{\circ}$  was associated with the type II burst and flare. The first appearance of the CME in the LASCO C2 field of view (FOV) was at  $\approx 07:48$  UT at a heliocentric distance of  $\approx 2.5 R_{\odot}$  in the sky plane. The average speed and residual acceleration of the CME in the combined LASCO C2 and C3 FOV were  $v_{\text{lasco}} \approx 679 \text{ km s}^{-1}$  and  $a_{\text{lasco}} \approx 6.2 \text{ m s}^{-2}$ . Similar information for all the 41 radio bursts are listed in Table 1. The date and time of occurrence ( $t_{\text{type II}}$  in hh:mm format) of the type II bursts considered in the present study are listed in Columns 2 and 3. Their projected radial distance ( $r_{\text{type II}}$ ) and position angle are given in Columns 4 and 5. The error in the estimated type II burst location is  $\approx \pm 0.2 R_{\odot}$  and is primarily due to the angular resolution of the GRH. Details of the associated GOES soft X-ray flares like the onset time ( $t_{\text{flareO}}$ ), time of occurrence of the peak ( $t_{\text{flareP}}$ ), and the flare class are given in Columns 6 and 7. The heliographic coordinates of the flare locations are given in Column 8. The first-appearance time/height of the associated CMEs, their CPA and width, speed and residual acceleration (all in the combined LASCO FOV) are given in Columns 9–12, respectively.

The shift in the solar radio source position due to ionospheric effects is expected to be  $\lesssim 0.1 R_{\odot}$  at 80 MHz in the hour angle range  $\pm 2$  hr (Stewart & McLean 1982). At 109 MHz, the error is expected to be even smaller since the refraction varies as  $f^{-2}$  where  $f$  is the observing frequency. Similarly, the effects of scattering (irregular refraction due to density inhomogeneities in the solar corona) on the observed source position/height are also considered to be small ( $< 0.2 R_{\odot}$ ) at 109 MHz compared to lower frequencies (Aubier et al. 1971; Riddle 1974; Robinson 1983; Thejappa et al. 2007). In either case the possible shift in position is within the error (i.e.,  $\pm 0.2 R_{\odot}$ ) in the estimated type II burst location mentioned in the previous paragraph. Ray tracing calculations employing realistic coronal electron density models and density fluctuations show that the turning points of the rays that undergo irregular refraction almost coincide with the location of the plasma (“critical”) layer in the non-scattering case even at 73.8 MHz (Thejappa & MacDowall 2008). Obviously, the situation should be better still at 109 MHz. Moreover, source sizes smaller than that predicted by the scattering theory have been observed (Ramesh et al. 2012). Note that there is no unambiguous evidence that scattering is important in any of the solar radio bursts (McLean & Melrose 1985). Lifting of the source centroid to a larger radial distance due to wave ducting (Duncan 1979) can be ruled out in the present case since the projected radial distances of 39/41 type II bursts ( $r_{\text{type II}}$ ) reported in this paper (see Column 4 in Table 1) are close to the radial distance of the 109 MHz plasma level ( $\approx 1.2 R_{\odot}$ ) in the “background” corona (Newkirk 1961) within nearly  $\pm 0.2 R_{\odot}$  (the error in the position of the type II burst mentioned above). We do not expect ducting to play a role in the remaining 2/41 cases alone. An inspection of SGD indicates that all the type II bursts at 109 MHz considered for the present study are harmonic components. This is expected since the fundamental component in the case of the type II bursts close to the solar limb may be occulted by the overlying corona and hence do not reach the observer (Nelson & Melrose 1985). The directivity of the fundamental emission is limited as compared to that of the harmonic (Thejappa et al. 2007, 2012). We would like to note here that the observed emission being harmonic further reduces (by a factor of  $\approx 2$ ) the possible shift in the source position due to scattering and other refraction effects in the solar corona (Thejappa et al. 2007, 2011).

<sup>7</sup> [http://www.lmsal.com/solarsoft/latest\\_events/](http://www.lmsal.com/solarsoft/latest_events/)

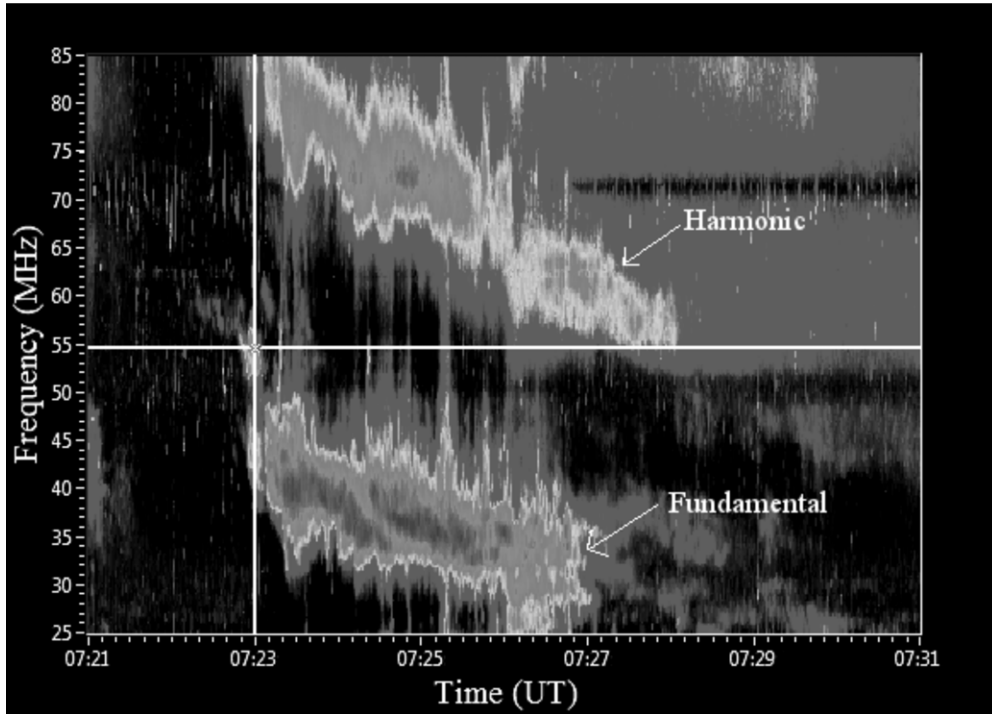


**Figure 2.** Dynamic spectrum of the type II radio burst of 2007 May 23 observed with the low-frequency radio spectrograph in the Gauribidanur observatory. The horizontal “white” line on the spectrum corresponds to 54.5 MHz, the fundamental component of the type II burst whose harmonic was observed with the GRH at 109 MHz (see Figure 1). The vertical “white” line on the spectrum corresponds to  $\approx 07:23$  UT, the time at which the type II burst was observed at 54.5 MHz (in the above spectrum) and 109 MHz (in Figure 1).

### 3. ANALYSIS AND RESULTS

From the existing literature we find that (1) the time period over which the initial CME acceleration takes place is synchronized with the rise time (onset-peak) of the associated *GOES* soft X-ray flare (Zhang et al. 2001, 2004; Neupert et al. 2001; Alexander et al. 2002; Gallagher et al. 2003; Shanmugaraju et al. 2003; Temmer et al. 2010) and usually continues up to  $\approx 10$  m after the flare maximum (Maričić et al. 2007), (2) the velocity ( $v$ ) of the CME at the end of the initial acceleration phase is close to the average velocity seen in the LASCO C2 and C3 FOV (Zhang & Dere 2006), and (3) the CME dynamics is closely related to the energetics of the soft X-ray flare (Hundhausen 1997; Moon et al. 2003; Burkepile et al. 2004; Vršnak et al. 2005; Aarnio et al. 2011; Shanmugaraju et al. 2011). Therefore, one can estimate the initial acceleration ( $a_{\text{ini}}$ ) using the kinematic equation  $v = u + a\Delta t$  as mentioned in Zhang & Dere (2006) and Gopalswamy et al. (2012b). Here  $u$  is the initial CME velocity,  $a = a_{\text{ini}}$ , and  $\Delta t = t_{\text{flareP}} - t_{\text{flareO}}$  as mentioned earlier. We assumed  $u = 0$  since the CME is considered to start from rest as it erupts (Lin et al. 2006; Gopalswamy et al. 2009a), and the source region of the CMEs to be the same as the location of the corresponding flares. The acceleration values estimated using the above equation are listed in Column 5 of Table 2. The values are in the range of initial CME acceleration over  $r \lesssim 2 R_{\odot}$  reported by various authors (St. Cyr et al. 1999; Alexander et al. 2002; Gallagher et al. 2003; Shanmugaraju et al. 2003; Zhang et al. 2004; Zhang & Dere 2006; Vršnak et al. 2007; Gopalswamy & Thompson 2000; Gopalswamy et al. 2009a, 2012a, 2012b; Temmer et al. 2008, 2010; Ramesh et al. 2010; Bein et al. 2011).

Assuming that the metric type II bursts observed in association with the CMEs are due to shock driven by the latter during their initial acceleration phase (Neupert et al. 2001; Cliver et al.

2004), we estimated the distance ( $s$ ) traveled by the CMEs (from the flare site) using the kinematic equation,  $s = ut + 0.5a\delta t^2$ . Here,  $a = a_{\text{ini}}$  mentioned above and  $\delta t$  is the time interval between the onset of the associated *GOES* soft X-ray flare ( $t_{\text{flare}}$  in Column 6 of Table 1) and the type II burst ( $t_{\text{typeII}}$  in Column 3 of Table 1). Adding the  $s$  values thus obtained to the projected radial distance of the corresponding flares ( $r_{\text{flare}}$  in Column 4 of Table 2), we get the projected radial distance of the CME ( $r_{\text{cme}}$  in Column 6 of Table 2). The separation between the position of the metric type II burst and  $r_{\text{cme}}$ , i.e.,  $r_{\text{typeII}} - r_{\text{cme}}$ , is given in Column 7 of Table 2. Considering the event of 2007 May 23 in Figure 1, we find that the flare onset  $t_{\text{flare}} \approx 07:15$  UT. The projected  $r_{\text{flare}}$  is  $\approx 0.8 R_{\odot}$ . The appearance of the type II burst at 109 MHz ( $t_{\text{typeII}}$ ) was at  $\approx 07:23$  UT. This implies that in the present case,  $\delta t \approx 480$  s. The estimated initial CME acceleration is  $a_{\text{ini}} \approx 666 \text{ m s}^{-2}$ . Substituting the values in the above kinematic equation, we get the distance traveled by the associated CME from the flare site in the time interval  $\delta t$  as  $s \approx 0.1 R_{\odot}$ . Adding this to  $r_{\text{flare}}$ , we get projected  $r_{\text{cme}} \approx 0.9 R_{\odot}$ . This is close to the height ( $\approx 0.5 R_{\odot}$ ) of the CME obtained around the same time ( $\approx 07:23$  UT) from EUV observations (Bein et al. 2011). The peak acceleration of the CME derived by the above authors from numerical differentiation of the CME height–time data is  $\approx 300 \text{ m s}^{-2}$ . The radial distance of the metric type II burst observed in association with the aforementioned flare and the CME is  $r_{\text{typeII}} \approx 1.4 R_{\odot}$ . This indicates that the type II burst position is ahead of the leading edge (LE) of the associated CME by  $\approx 0.5 R_{\odot}$  (Column 7 in Table 2). The difference between the CPA of the CME LE ( $\text{CPA}_{\text{cme}}$ ) and the type II radio burst ( $\text{CPA}_{\text{typeII}}$ ) is  $\approx 4^{\circ}$  (see Column 8 in Table 2). In a similar manner we estimated  $r_{\text{cme}}$  for the other CMEs in Table 1. Comparing the  $r_{\text{cme}}$  for each CME in the present case with the  $r_{\text{typeII}}$  of the corresponding type II bursts, we find that  $r_{\text{typeII}} \geq r_{\text{cme}}$  in

**Table 1**  
Details of the Metric Type II Bursts and the Associated Flares, CMEs

No.	Date	Type II Burst at 109 MHz			GOES X-Ray and H $\alpha$ Flare Details			SOHO–LASCO CME Details			
		Time $t_{\text{type II}}$ (UT)	Proj. $r_{\text{type II}}$ ( $R_{\odot}$ )	CPA (deg.)	Onset/Peak $t_{\text{flare O}}$ / $t_{\text{flare P}}$ (UT)	X-Ray Class	H $\alpha$ Posn	Time (UT)/ Distance ( $R_{\odot}$ ) <sup>a</sup>	CPA/ Width (deg.) <sup>a</sup>	Speed $v_{\text{lasco}}$ ( $\text{km s}^{-1}$ ) <sup>b</sup>	Residual Accln $a_{\text{lasco}}$ ( $\text{m s}^{-2}$ ) <sup>c</sup>
(1)	(2)	(3)	(4)	(5)	(6)	(7)	(8)	(9)	(10)	(11)	(12)
1	1997 May 12	04:52	0.9	296	04:42/04:55	C1.3	N21W08	06:30/6.2	268/67	464	−15.0
2	1997 Nov 4	05:59	1.1	262	05:52/05:58	X2.1	S14W33	06:10/2.7	251/53	785	−22.1
3	1998 Apr 23	05:38	1.3	113	05:35/05:55	X1.2	S17E91	05:55/4.4	105/98	1691	−44.4
4	1999 Mar 8	06:39	1.3	85	06:30/06:43	M2.6	S24E93	06:54/2.3	112/79	664	−10.0
5	1999 May 3	05:42	0.9	36	05:36/06:02	M4.4	N15E32	06:06/3.3	50/100	1584	15.8
6	2000 Feb 12	04:00	0.9	316	03:51/04:10	M1.7	N26W23	04:31/3.3	330/60	1107	−8.3
7	2000 Apr 12	06:35	0.9	270	06:22/06:30	C2.1	S19W28	07:31/2.8	254/25	425	−26.5
8	2000 Apr 30	08:01	1.1	201	07:53/08:08	C7.7	S11W18	08:54/3.2	197/40	540	7.3
9	2000 May 20	05:57	0.8	200	05:50/06:00	C7.6	S15W08	06:26/2.7	236/40	557	−5.3
10	2000 Jun 1	07:38	0.9	104	07:28/07:32	C8.2	S14E24	08:06/3.1	106/21	603	103.2
11	2000 Jun 23	04:12	1.1	308	04:00/04:07	M2.6	N19W30	04:54/2.6	306/78	460	56.3
12	2000 Jun 25	07:49	1.4	262	07:32/07:52	M1.9	N16W55	07:54/2.7	271/39	1617	−17.5
13	2000 Aug 25	07:48	1.0	76	07:31/07:46	C1.7	S17E69	08:06/1.4	89/30	330	18
14	2000 Sep 9	08:39	1.1	305	08:28/08:49	M1.6	N07W67	08:56/3.2	284/57	554	−13.4
15	2000 Sep 15	05:11	1.3	298	05:05/05:32	M2.1	N13W00	05:50/3.5	298/37	155	−2.3
16	2000 Sep 16	04:10	1.4	274	04:06/04:26	M5.9	N14W07	05:18/9.0	287/77	1215	−12.3
17	2000 Oct 3	07:46	1.2	341	07:40/07:46	C1.5	N27W59	08:06/3.3	318/42	434	−5.2
18	2000 Nov 14	08:08	1.1	106	07:52/08:06	C7.1	S26E65	08:30/2.6	123/45	408	−0.4
19	2001 Jan 26	06:04	1.3	67	05:53/06:07	M1.0	N10E63	06:30/3.0	83/35	314	1.5
20	2001 Oct 9	07:40	1.3	280	07:24/07:41	C7.0	N19E67	08:06/2.8	272/73	526	−2.1
21	2001 Oct 11	04:28	1.3	56	04:12/04:25	C4.6	N22E47	04:54/3.0	57/67	677	−12.8
22	2001 Oct 13	05:30	1.0	85	05:19/05:23	C5.3	S19E34	05:54/3.1	104/24	546	−0.3
23	2001 Nov 17	04:51	1.1	93	04:49/05:25	M2.8	S13E42	05:30/5.8	75/150	1379	−22.5
24	2004 Jan 20	07:46	1.2	165	07:29/07:43	M6.1	S15W13	08:30/4.0	185/95	590	...
25	2004 Apr 5	05:52	1.3	100	05:37/05:55	M1.7	S16E26	06:06/2.7	124/40	608	−9.7
26	2004 Jun 16	04:24	1.6	70	04:15/04:34	C2.8	S08E81	04:36/2.7	81/72	603	−2.0
27	2004 Jul 12	08:08	1.4	88	07:36/08:08	M1.6	S08E90	08:06/2.7	77/91	610	−11
28	2004 Aug 31	05:41	1.3	266	05:24/05:38	M1.4	N06W82	05:54/2.4	273/45	311	−3.4
29	2004 Oct 30	06:17	1.3	270	06:08/06:18	M4.2	N13W22	06:54/3.4	263/69	422	25.9
30	2004 Oct 31	05:39	1.3	274	05:23/05:32	M2.3	N12W36	06:30/2.9	268/67	265	7.6
31	2005 Jan 15	05:57	1.1	14	05:54/06:38	M8.6	N16E04	06:30/5.8	1/118	2049	−30.7
32	2005 Jan 19	08:16	1.3	300	08:03/08:22	X1.3	N19W47	08:29/4.5	321/70	2020	−43.8
33	2005 Jan 20	06:50	1.3	300	06:36/07:01	X7.1	N14W61	06:54/4.1	292/85	882	16
34	2005 Mar 19	07:10	1.2	248	06:56/07:07	C2.3	S09W52	07:36/2.4	246/24	369	12.9
35	2005 Jul 1	05:05	1.2	85	04:57/05:02	C5.3	N14E83	05:30/3.3	79/36	419	−23.1
36	2005 Jul 27	04:47	1.4	100	04:33/05:02	M3.7	N11E90	04:54/2.9	84/75	1787	−75.4
37	2005 Jul 28	06:27	1.9	60	06:13/06:37	C2.8	N11E81	06:54/3.0	72/31	573	−8.1
38	2005 Jul 30	06:32	1.5	71	06:17/06:35	X1.3	N12E60	06:50/5.7	50/106	1968	−102.6
39	2005 Aug 3	05:08	1.4	100	04:54/05:06	M3.4	S13E45	05:30/2.7	123/25	479	−6.7
40	2006 Jul 6	08:26	1.3	279	08:13/08:51	M2.5	S09W34	08:54/2.8	233/89	911	8.2
41	2007 May 23	07:23	1.4	262	07:15/07:32	B5.3	S10W51	07:48/2.5	266/72	679	6.2

**Notes.**<sup>a</sup> At the first appearance in the SOHO–LASCO FOV.<sup>b</sup> Based on quadratic fit to the height–time measurements.<sup>c</sup> Based on linear fit to the height–time measurements.

38/41 cases. Note that we have taken into consideration the error in the position of type II bursts ( $\approx \pm 0.2 R_{\odot}$ ) as mentioned in Section 2 in declaring the above statistics. The maximum distance by which the CME LE was ahead of the type II radio burst position was  $\approx 1.1 R_{\odot}$ . However for a majority of the events (32/38) the separation was  $\lesssim 0.5 R_{\odot}$  (see Column 7 in Table 2). These numbers are consistent with the standoff distance ( $\lesssim 1 R_{\odot}$ ) from the LE of the CME where the shock is expected (Gopalswamy & Kundu 1992; Gopalswamy et al. 2012a). In the remaining 3/41 cases, the type II burst is behind the LE of the corresponding CME by  $< 0.5 R_{\odot}$ . This separation is less than the thickness ( $\approx 1 R_{\odot}$ ) of the frontal structure of a CME (Gopalswamy 1999).

We also estimated  $r_{\text{cme}}$  from the initial acceleration of the CMEs calculated using the relation  $a_{\text{ini}} = 4.2 \times 10^6 w + 600$ , where  $w$  is the flux of the associated GOES soft X-ray flare (Ramesh et al. 2010). The results are consistent with the corresponding values in Table 2.

We also find that (1) the  $r_{\text{type II}}$  values in 39/41 cases (see Column 3 in Table 2) agree with the recent results that the MHD fast-mode shocks leading to metric type II radio bursts form low in the corona, at a distance of  $r < 1.5 R_{\odot}$  (Gopalswamy et al. 2009a, 2012a; Magdalenic et al. 2010); (2) the projected  $r_{\text{cme}}$  values in 38/41 cases (see Column 6 in Table 2) agree with the reports that the CMEs reach their maximum acceleration

**Table 2**  
Details of Some of the Estimated Values for the Type II Bursts,  
Associated Flares and CMEs

No.	Date	Proj. $r_{\text{type II}}$ ( $R_{\odot}$ )	Proj. $r_{\text{flare}}$ ( $R_{\odot}$ )	Accln $a_{\text{ini}}$ ( $\text{m s}^{-2}$ )	Proj. $r_{\text{cme}}$ ( $R_{\odot}$ )	$r_{\text{type II}}$ $- r_{\text{cme}}$ ( $R_{\odot}$ ) <sup>a</sup>	$\text{CPA}_{\text{cme}}$ – $\text{CPA}_{\text{type II}}$ (deg)
(1)	(2)	(3)	(4)	(5)	(6)	(7)	(8)
1	1997 May 12	0.9	0.4	595	0.6	0.3	–28
2	1997 Nov 4	1.1	0.6	2180	0.9	0.2	–11
3	1998 Apr 23	1.3	1.0	1409	1.0	0.3	–8
4	1999 Mar 8	1.3	1.0	851	1.2	0.1	27
5	1999 May 3	0.9	0.6	1015	0.7	0.2	14
6	2000 Feb 12	0.9	0.6	971	0.8	0.1	14
7	2000 Apr 12	0.9	0.6	885	1.0	–0.1	–16
8	2000 Apr 30	1.1	0.4	600	0.5	0.6	–4
9	2000 May 20	0.8	0.3	928	0.4	0.4	36
10	2000 Jun 1	0.9	0.5	2512	1.1	–0.2	2
11	2000 Jun 23	1.1	0.6	1095	1.0	0.1	–2
12	2000 Jun 25	1.4	0.8	1348	1.8	–0.4	9
13	2000 Aug 25	1.0	0.9	367	1.2	–0.2	13
14	2000 Sep 9	1.1	0.9	440	1.0	0.1	–21
15	2000 Sep 15	1.3	0.2	96	0.2	1.1	0
16	2000 Sep 16	1.4	0.3	1013	0.3	1.1	13
17	2000 Oct 3	1.2	0.9	1206	1.0	0.2	–23
18	2000 Nov 14	1.1	0.9	486	1.2	–0.1	17
19	2001 Jan 26	1.3	0.9	642	1.0	0.3	16
20	2001 Oct 9	1.3	0.9	516	1.2	0.1	–8
21	2001 Oct 11	1.3	0.8	868	1.4	–0.1	1
22	2001 Oct 13	1.0	0.6	2275	1.2	–0.2	19
23	2001 Nov 17	1.1	0.7	638	0.7	0.4	–18
24	2004 Jan 20	1.2	0.3	702	0.8	0.4	20
25	2004 Apr 5	1.3	0.5	563	0.8	0.5	24
26	2004 Jun 16	1.6	1.0	529	1.1	0.5	11
27	2004 Jul 12	1.4	1.0	318	1.8	–0.4	–11
28	2004 Aug 31	1.3	1.0	370	1.3	0.0	7
29	2004 Oct 30	1.3	0.4	703	0.6	0.7	–7
30	2004 Oct 31	1.3	0.6	491	0.9	0.4	–6
31	2005 Jan 15	1.1	0.3	776	0.3	0.8	–13
32	2005 Jan 19	1.3	0.8	1771	1.5	–0.2	21
33	2005 Jan 20	1.3	0.9	588	1.2	0.1	–8
34	2005 Mar 19	1.2	0.8	559	1.1	0.1	–2
35	2005 Jul 1	1.2	1.0	1397	1.2	0.0	–6
36	2005 Jul 27	1.4	1.0	1027	1.5	–0.1	–16
37	2005 Jul 28	1.9	1.0	398	1.2	0.7	12
38	2005 Jul 30	1.5	0.9	1822	1.9	–0.4	–21
39	2005 Aug 3	1.4	0.7	665	1.0	0.4	23
40	2006 Jul 6	1.3	0.6	400	0.8	0.5	–46
41	2007 May 23	1.4	0.8	666	0.9	0.5	4

**Note.** <sup>a</sup> Positive  $r_{\text{type II}} - r_{\text{cme}}$  indicates that the type II burst is located at or above the LE of the associated CME and vice versa.

within  $r < 1.5 R_{\odot}$  (Alexander et al. 2002; Gallagher et al. 2003; Vrřnak et al. 2007; Temmer et al. 2008, 2010; Bein et al. 2011); and (3) all the type II bursts were located within  $\pm 45^{\circ}$  from the CPA of the CME LE (see Column 8 in Table 2). Note that statistical studies show that the mean width of the CMEs associated with the metric type II bursts is  $\approx 90^{\circ}$  (Lara et al. 2003). We would like to note here that for the 3/41 events for which  $r_{\text{type II}}$  is behind  $r_{\text{cme}}$  the maximum separation is  $\approx 0.4 R_{\odot}$  (see Column 7 in Table 2). This is less than  $r \approx 1.5 R_{\odot}$ , the radial distance below which the maximum acceleration of CMEs and MHD shocks leading to metric type II bursts are expected to occur. These indicate that the metric type II bursts reported in the present work might be due to shocks driven by the associated CMEs.

The initial CME acceleration over  $r \lesssim 2 R_{\odot}$  is generally significantly different from that obtained with the CME LE height–time measurements at larger distances ( $r > 2 R_{\odot}$ ) using LASCO C2 and C3 coronagraphs. This is because the above instruments do not “see” the initial acceleration phase of the CMEs due to FOV restrictions. They see only the residual acceleration (Zhang & Dere 2006). If we use the *SOHO*/LASCO catalog acceleration ( $a_{\text{LASCO}}$ ), i.e., the residual CME acceleration, in the kinematic equation mentioned in the previous paragraph, we find that the type II bursts generally occur after CMEs have crossed the type II location, which might lead to the conclusion that  $r_{\text{type II}}$  is behind the CME LE at  $t_{\text{type II}}$ . However, when we compute  $r_{\text{type II}}$  using  $a_{\text{ini}}$  mentioned above, we find that  $r_{\text{type II}}$  is either at or above the CME LE at  $t_{\text{type II}}$ .

#### 4. CONCLUSIONS

We studied 41 metric type II radio bursts observed with the GRH during the period 1997–2007. These events were located close to the solar limb ( $r \gtrsim 0.8 R_{\odot}$ ). We calculated the position of the CME LE at the time of appearance of the associated type II bursts in a straightforward manner using simple kinematic equations. Neither any coronal density model was assumed nor Sunward extrapolation of the height–time measurements of the white-light CMEs observed at larger distances from the Sun was used. We find that in 38/41 events considered for the study, the position of the metric type II radio burst was either at or above the LE of the associated CME. For three events, the type II burst was behind the CME LE by  $< 0.5 R_{\odot}$ . This separation is less than the typical thickness ( $\approx 1 R_{\odot}$ ) of the frontal structure of a CME. We repeated the calculations using the relationship between the initial acceleration of a CME in the low corona and the flux of the associated *GOES* soft X-ray flare published in the literature. The results were consistent. In summary, our results indicate that metric type II bursts reported in this paper are most likely due to MHD shocks driven by the associated CMEs.

We acknowledge the staff of the Gauribidanur radio observatory for their help in data collection and maintenance of the antenna and receiver systems there. We are grateful to A. O. Benz for kindly donating a CALLISTO radio spectrograph to the Indian Institute of Astrophysics, and C. Monstein for installing the same in Gauribidanur. The work reported in this paper was carried out when M.A.L. was a Visiting Intern at the Indian Institute of Astrophysics, Bangalore during 2011 August. We thank the referee for his/her help to bring out the results more clearly. The *SOHO* data are produced by a consortium of the Naval Research Laboratory (USA), Max-Planck-Institut für Aeronomie (Germany), Laboratoire d’Astronomie (France), and the University of Birmingham (UK). *SOHO* is a project of international cooperation between ESA and NASA.

#### REFERENCES

- Aarnio, A. N., Stassun, K. G., Hughes, W. J., & McGregor, S. L. 2011, *Sol. Phys.*, **268**, 195  
 Alexander, D., Metcalf, T. R., & Nitta, N. V. 2002, *Geophys. Res. Lett.*, **29**, 41  
 Aubier, M., Leblanc, Y., & Boischoat, A. 1971, *A&A*, **12**, 435  
 Aurass, H. 1997, in *Coronal Physics from Radio and Space Observations*, ed. G. Trotter (Lecture Notes in Physics; Berlin: Springer), 135  
 Bein, B. M., Berkebile-Stoiser, B., Veronig, A. M., et al. 2011, *ApJ*, **738**, 191  
 Benz, A. O., Monstein, C., & Meyer, H. 2005, *Sol. Phys.*, **226**, 121  
 Brueckner, G. E., Howard, R. A., Koomen, M. J., et al. 1995, *Sol. Phys.*, **162**, 357  
 Burkepile, J. T., Hundhausen, A. J., Stanger, A. L., St. Cyr, O. C., & Seiden, J. A. 2004, *J. Geophys. Res.*, **109**, A03103

- Cho, K.-S., Bong, S.-C., Kim, Y.-H., et al. 2008, *A&A*, **491**, 873
- Cho, K.-S., Bong, S.-C., Moon, Y.-J., et al. 2011, *A&A*, **530**, A16
- Cho, K.-S., Lee, J., Moon, Y.-J., et al. 2007, *A&A*, **461**, 1121
- Cho, K.-S., Moon, Y.-J., Dryer, M., et al. 2005, *J. Geophys. Res.*, **110**, A12101
- Cliver, E. W., Nitta, N. V., Thompson, B. J., & Zhang, J. 2004, *Sol. Phys.*, **225**, 105
- Cliver, E. W., Webb, D. F., & Howard, R. A. 1999, *Sol. Phys.*, **187**, 89
- Delaboudiniere, J.-P., Artzner, G. E., Brunaud, J., et al. 1995, *Sol. Phys.*, **162**, 291
- Dulk, G. A. 1970, *Proc. Astron. Soc. Aust.*, **1**, 308
- Duncan, R. A. 1979, *Sol. Phys.*, **63**, 389
- Ebenezer, E., Subramanian, K. R., Ramesh, R., Sundara Rajan, M. S., & Kathiravan, C. 2007, *Bull. Astron. Soc. India*, **35**, 111
- Gallagher, P. T., Lawrence, G. R., & Dennis, B. R. 2003, *ApJ*, **588**, L53
- Gary, D. J., Dulk, G. A., House, L., et al. 1984, *A&A*, **134**, 222
- Gergely, T. E., Kundu, M. R., & Hildner, E. 1983, *ApJ*, **268**, 403
- Gopalswamy, N. 1999, in *Proc. Nobeyama Symp., Solar Physics with Radio Observations*, ed. T. Bastian, N. Gopalswamy, & K. Shibasaki (NRO Report 479; Nobeyama: NRO), 141
- Gopalswamy, N. 2006, in *Solar Eruptions and Energetic Particles*, ed. N. Gopalswamy, R. Mewaldt, & J. Torsti (Geophysics Monograph Series 165; Washington, DC: AGU), 207
- Gopalswamy, N., & Kundu, M. R. 1992, in *AIP Conf. Ser. 264, Particle Acceleration in Cosmic Plasmas*, ed. G. P. Zank & T. K. Gaisser (Melville, NY: AIP), 257
- Gopalswamy, N., Lara, A., Kaiser, M. L., & Bougeret, J.-L. 2001, *J. Geophys. Res.*, **106**, 25261
- Gopalswamy, N., Nitta, N. V., Akiyama, S., Mäkelä, P., & Yashiro, S. 2012a, *ApJ*, **744**, 72
- Gopalswamy, N., & Thompson, B. J. 2000, *J. Atmos. Sol.-Terr. Phys.*, **62**, 1457
- Gopalswamy, N., Thompson, W. T., Davila, J. M., et al. 2009a, *Sol. Phys.*, **259**, 227
- Gopalswamy, N., Xie, H., Yashiro, S., et al. 2012b, *Space Sci. Rev.*, in press (arXiv:1205.0688)
- Gopalswamy, N., Yashiro, S., Michalek, G., et al. 2009b, *Earth Moon Planets*, **104**, 295
- Hundhausen, A. J. 1997, in *Coronal Mass Ejections*, ed. N. Crooker, J. A. Joselyn, & J. Feynman (Geophysics Monograph Series 99; Washington, DC: AGU), 1
- Kosugi, T. 1976, *Sol. Phys.*, **48**, 339
- Lara, A., Gopalswamy, N., Nunes, S., Muñoz, G., & Yashiro, S. 2003, *Geophys. Res. Lett.*, **30**, 816
- Lin, J., Mancuso, S., & Vourlidas, A. 2006, *ApJ*, **649**, 1110
- Liu, Y., Luhmann, J. G., Bale, S. D., & Lin, R. P. 2009, *ApJ*, **691**, L151
- Maia, D., Pick, M., Vourlidas, A., & Howard, R. 2000, *ApJ*, **528**, L49
- Magdalenic, J., Marqué, C., Zhukov, A. N., Vršnak, B., & Žic, T. 2010, *ApJ*, **718**, 266
- Mann, G., Classen, T., & Aurass, H. 1995, *A&A*, **295**, 775
- Mann, G., & Vršnak, B. 2007, in *Recent Research: Large-scale Disturbances, Their Origin and Consequences*, ed. G. Trottet (Lecture Notes in Physics; Berlin: Springer), 203
- Mancuso, S. 2007, *A&A*, **463**, 1137
- Maričić, D., Vršnak, B., Stanger, A. L., et al. 2007, *Sol. Phys.*, **241**, 99
- McLean, D. J., & Melrose, D. B. 1985, in *Solar Radiophysics*, ed. D. J. McLean & N. R. Labrum (Cambridge: Cambridge Univ. Press), 237
- Monstein, C., Ramesh, R., & Kathiravan, C. 2007, *Bull. Astron. Soc. India*, **35**, 473
- Moon, Y.-J., Choe, G. S., Wang, H., Park, Y. D., & Cheng, C. Z. 2003, *J. Korean. Astron. Soc.*, **36**, 61
- Nelson, G. J., & Melrose, D. B. 1985, in *Solar Radiophysics* (Cambridge: Cambridge Univ. Press), 333
- Nelson, G. J., & Robinson, R. D. 1975, *Proc. Astron. Soc. Aust.*, **2**, 370
- Neupert, W. M., Thompson, B. J., Gurman, J. B., & Plunkett, S. P. 2001, *J. Geophys. Res.*, **106**, 25215
- Newkirk, G. 1961, *ApJ*, **133**, 983
- Nindos, A., Alissandrakis, C. E., Hillaris, A., & Preka-Papadema, P. 2011, *A&A*, **531**, A31
- Pick, M., & Vilmer, N. 2008, *A&AR*, **16**, 1
- Ramesh, R., Kathiravan, C., Barve, I. V., & Rajalingam, M. 2012, *ApJ*, **744**, 165
- Ramesh, R., Kathiravan, C., Kartha, S. S., & Gopalswamy, N. 2010, *ApJ*, **712**, 188
- Ramesh, R., Subramanian, K. R., SundaraRajan, M. S., & Sastry, Ch. V. 1998, *Sol. Phys.*, **181**, 439
- Riddle, A. C. 1974, *Sol. Phys.*, **35**, 153
- Robinson, R. D. 1983, *Proc. Astron. Soc. Aust.*, **5**, 208
- Shanmugaraju, A., Moon, Y.-J., Dryer, M., & Umopathy, S. 2003, *Sol. Phys.*, **215**, 185
- Shanmugaraju, A., Moon, Y.-J., & Vršnak, B. S. 2011, *Sol. Phys.*, **270**, 273
- St. Cyr, O. C., Burkepile, J. T., Hundhausen, A. J., & Lecinski, A. R. 1999, *J. Geophys. Res.*, **104**, 12493
- Stewart, R. T., Howard, R. A., Hansen, F., Gergely, T., & Kundu, M. R. 1974a, *Sol. Phys.*, **36**, 219
- Stewart, R. T., McCabe, M. K., Koomen, M. J., Hansen, R. T., & Dulk, G. A. 1974b, *Sol. Phys.*, **36**, 203
- Stewart, R. T., & McLean, D. J. 1982, *Proc. Astron. Soc. Aust.*, **4**, 386
- Subramanian, K. R., & Ebenezer, E. 2006, *A&A*, **451**, 683
- Temmer, M., Veronig, A. M., Kontar, E. P., Krucker, S., & Vršnak, B. 2010, *ApJ*, **712**, 1410
- Temmer, M., Veronig, A. M., Vršnak, B., et al. 2008, *ApJ*, **673**, L95
- Thejappa, G., & MacDowall, R. J. 2008, *ApJ*, **676**, 1338
- Thejappa, G., MacDowall, R. J., & Bergamo, M. 2012, *ApJ*, **745**, 187
- Thejappa, G., MacDowall, R. J., & Gopalswamy, N. 2011, *ApJ*, **734**, 16
- Thejappa, G., MacDowall, R. J., & Kaiser, M. L. 2007, *ApJ*, **671**, 894
- Vršnak, B., & Cliver, E. W. 2008, *Sol. Phys.*, **253**, 215
- Vršnak, B., Maričić, D., Stanger, A. L., et al. 2007, *Sol. Phys.*, **241**, 85
- Vršnak, B., Sudar, D., & Ruždak, D. 2005, *A&A*, **435**, 1149
- Wagner, W. J., & MacQueen, R. M. 1983, *A&A*, **120**, 136
- Zhang, J., & Dere, K. P. 2006, *ApJ*, **649**, 1100
- Zhang, J., Dere, K. P., Howard, R. A., Kundu, M. R., & White, S. M. 2001, *ApJ*, **559**, 452
- Zhang, J., Dere, K. P., Howard, R. A., & Vourlidas, A. 2004, *ApJ*, **604**, 420